Carbohydrate Polymers 75 (2009) 1–8

Contents lists available at ScienceDirect

Carbohydrate Polymers

journal homepage: www.elsevier.com/locate/carbpol

Properties of biodegradable citric acid-modified granular starch/thermoplastic pea starch composites

Xiaofei Ma [a], Peter R. Chang [b,c,*], Jiugao Yu [a], Mark Stumborg [b]

[a] School of Science, Tianjin University, Tianjin 300072, China
[b] Bioproducts and Bioprocesses National Science Program, Agriculture and Agri-Food Canada, 107 Science Place, Saskatoon, SK, Canada S7N 0X2
[c] Department of Agricultural and Bioresource Engineering, University of Saskatchewan, Saskatoon, SK, Canada S7N 5A9

ARTICLE INFO

Article history:
Received 8 May 2008
Received in revised form 21 May 2008
Accepted 27 May 2008
Available online 5 June 2008

Keywords:
Pea starch
Rice starch
Citric acid
Composites

ABSTRACT

Pea starch-based composites reinforced with citric acid-modified pea starch (CAPS) and citric acid-modified rice starch (CARS), respectively, were prepared by screw extrusion. The effects of granular CAPS and CARS on the morphology, thermal stability, dynamic mechanical thermal analysis, the relationship between the mechanical properties and water content, as well as the water vapor permeability of the composite films were investigated. Scanning electron microscope and X-ray diffraction reveal that the reinforcing agents, the granules of CAPS and CARS, are not disrupted in the thermoplastic process, while the pea starch in the matrix is turned into a continuous TPS phase. Granular CAPS and CARS can improve the storage modulus, the glass transition temperature, the tensile strength and the water vapor barrier, but decrease thermal stability. CARS/TPS composites exhibit a better storage modulus, tensile strength, elongation at break and water vapor barrier than CAPS/TPS composites because of the smaller size of the CARS granules.

1. Introduction

Mounting environmental and legislative pressure for reducing petroleum-based plastics waste, and rapid increases in the cost of petroleum, have primed the development of bio-based materials from renewable resources. Among the biopolymers, starch is considered to be one of the most promising materials for biodegradable plastics because of its universality, renewability, and low cost. Starch has been investigated widely for the potential manufacture of products such as water-soluble pouches for detergents and insecticides, flushable liners and bags, and medical delivery systems and devices (Fishman, Coffin, & Konstance, 2000). Native starch commonly exists in a granular structure, which can be processed into thermoplastic starch (TPS) under the high temperature and shear of melt extrusion. (Forssell, Mikkilä, & Moates, 1997; Ma, & Yu, 2004a). Unfortunately, TPS exhibits many disadvantages such as a strong hydrophilic character (water sensitivity) and poor mechanical properties compared to conventional polymers (Averous, & Boquillon, 2004), which make it unsatisfactory for applications such as packaging materials. Generally, there are two approaches to mitigate these shortcomings. One approach is to blend starch with biodegradable polymers such as polylactide, polycaprolactone (Sarazin, Li, & Orts, 2008), and poly(propylene carbonate) (Ma, Yu, & Zhao, 2006). However, these polymers are very expensive, and starch is immiscible with them at the molecular level. The other approach is the reinforcement of TPS with mineral, cellulose or starch nanocrystal fillers. A significant improvement in mechanical properties and water resistance of TPS has been reported by such reinforcement. Mineral fillers such as kaolin (de Carvalho, Curvelo, & Agnelli, 2001) and clay (Park, Li, & Jin, 2002; Wilhelm, Sierakowski, & Souza, 2003) with polar groups were easily associated with TPS. Cellulose fillers used as reinforcing agents in TPS matrices include cellulose nanocrystals (Cao, Chen, Chang, Stumborg, & Huneault, in press; Lu, Weng, & Cao, 2006), natural fibers (Alvarez, Vázquez, & Bernal, 2005; Soykeabkaew, Supaphol, & Rujiravanit, 2004), cellulose derivatives (Ma, Chang, & Yu, 2008) and commercially regenerated cellulose fibers (Funke, Bergthaller, & Lindhauer, 1998). The chemical similarities of starch and plant fibers provide a sound basis for good interaction (Avérous, Fringant, & Moro, 2001; Lu et al., 2006). In addition, waxy maize starch nanocrystals, from the hydrolysis of native granules, have been used as a reinforcing agent in TPS prepared by casting (Angellier, Molina-Boisseau, & Dole, 2006). It is necessary to decrease the temperature of gelatinized starch before adding starch nanocrystals, otherwise the nanocrystals also gelatinize.

Pea starch is mainly available as a by-product of protein extraction. It is therefore considered to be a relatively cheap source of starch as compared to corn, wheat, and potato starches (Ratnayake,

* Corresponding author. Address: Bioproducts and Bioprocesses National Science Program, Agriculture and Agri-Food Canada, 107 Science Place, Saskatoon, SK, Canada S7N 0X2. Tel.: +1 306 9567637; fax: +1 306 9567247.
E-mail addresses: changp@agr.gc.ca, apogeec@shaw.ca (P.R. Chang).

0144-8617/$ - see front matter Crown copyright © 2008 Published by Elsevier Ltd. All rights reserved.
doi:10.1016/j.carbpol.2008.05.020

Hoover, & Warkentin, 2002). Citric acid (CA) is recognized as nutritionally harmless compared to other substances used for starch derivatization. (Xie & Liu, 2004). CA-modified starch is a granular resistant starch, which displays many of the physiological benefits of dietary fiber such as calorie reduction and colonic health benefits. These granules are not gelatinized during the processing of TPS, therefore CA-modified starch can be used as a reinforcing agent in TPS prepared by both melt extrusion and casting methods. In this paper, CA-modified pea starch (CAPS) and CA-modified rice starch (CARS) are used as reinforcing agents in glycerol-plasticized thermoplastic pea starch (TPS) matrices. This work is focused on the preparation and characterization of CAPS/TPS and CARS/TPS composites in terms of morphology, X-ray diffractometry, thermal stability, dynamic mechanical thermal analysis, and water vapor permeability, as well as the effect of water content on mechanical properties. This work also studied the size effect of reinforcing agents on the properties of the resultant composites as granules of rice starch are significantly smaller than those of pea starch. New applications for citric acid-modified granular starch as a reinforcement filler in starch-based biocomposites are explored in this work. These starch derivative/TPS composites may have great potential to replace conventional packaging such as edible films, food packaging, and biodegradable packaging.

2. Experimental

2.1. Materials

Pea starch (PS) composed of 35% amylose and 65% amylopectin was supplied by Nutri-Pea Limited Canada (Portage la Prairie, Canada). Rice starch (RS) containing 32% amylose and 68% amylopectin was obtained from Shanghai Starch Institute (Shanghai, China). Glycerol, the plasticizer, and citric acid (CA) were purchased from Tianjin Chemical Reagent Factory (Tianjin, China).

2.2. Production of CAPS and CARS

CAPS and CARS were produced based on the method of (Xie & Liu, 2004) with some modifications. CA (40 g) was dissolved in 100 mL of water and the pH of the solution was then adjusted to 3.5 with 10 M NaOH. The citric acid solution was mixed with 100 g dried PS or RS in a glass tray and stored for 12 h at room temperature. The tray was then dried at 60 °C for 6 h. The mixture was then ground and dried in a forced air oven for 1.5 h at 130 °C. The dry mixture was washed three times with water to remove unreacted CA. CAPS and CARS were air-dried at room temperature and finally ground.

2.3. The preparation of CAPS/TPS and CARS/TPS composites

Glycerol was blended (3000 rpm, 2 min) with pea starch and CAPS (or CARS) by use of a High Speed Mixer GH-100Y, and stored overnight. The ratio of glycerol to pea starch (wt/wt) was 30:100. The filler loading level (0, 3, 6, 9, or 12 wt%) was based on the pea starch. The mixtures were manually fed into a single screw Plastic Extruder SJ-25(s) (Screw Ratio L/D = 25:1) operating at 25 rpm. The temperature profile along the extruder barrel was based on four heating zones, 130, 140, 150, and 130 °C, from feed zone to die. The die was a round sheet with 3 mm diameter holes. Samples were pressed, using a flat sulfuration machine, into a sheet for testing.

2.4. Determination of the molar degree of substitution by CA

The molar degree of substitution (MS) is the number of CA per anhydroglucose unit (AGU) in starch. MS was determined using the method of Xing et al. (Xing, Zhang, & Ju, 2006) with minor modification. Approximately 1.0 g of dry CAPS or CARS was accurately weighed and placed into a 250 mL conical flask. Then 50 mL of 75% ethanol solution was added, and the conical flask was agitated and warmed at 50 °C for 30 min and then cooled to room temperature. Standard 0.500 M aqueous sodium hydroxide solution (20 mL) was added; the conical flask was tightly stoppered and agitated with a magnetic stirrer for 24 h. The excess alkali was back-titrated with a standard 0.200 M aqueous hydrochloric acid solution and re-titrated 2 h later to account for any further alkali that may have leached from the starch. Each sample was measured in triplicate. MS of CA substitution was 0.085 for CAPS and 0.089 for CARS.

2.5. Fourier transform infrared (FT-IR) spectroscopy

PS, RS, CAPS, CARS powders were measured with a BIO-RAD FTS3000 IR Spectrum Scanner.

2.6. Scanning electron microscope (SEM)

PS, RS, CAPS, CARS powders and the fracture surfaces of extruded composite strips were examined using a scanning electron microscope Philips XL-3, operating at an acceleration voltage of 20 kV. PS, RS, CAPS, CARS powders were suspended in ethanol. The suspension drops were drawn on a glass flake, dried to remove ethanol, and then vacuum coated with gold for SEM. Composite strips were cooled in liquid nitrogen, and then broken. The fracture faces were vacuum coated with gold for SEM.

2.7. X-ray diffractometry

The extruded composite strips were pressed at 10 MPa using a flat sulfuration machine and the slices were placed in a sample holder for X-ray diffractometry. PS, RS, CAPS, CARS powders were tightly packed into the sample holder. X-ray diffraction patterns were recorded in the reflection mode in angular range 10–30° (2 theta) at ambient temperature by a BDX3300 diffractometer, operated at the CuKα wavelength of 1.542 Å. Radiation from the anode, operated at 36 kV and 20 mA, monochromized with a 15 μm nickel foil. The diffractometer was equipped with 1° divergence slit, a 16 mm beam bask, a 0.2 mm receiving slit and a 1° scatter slit. Radiation was detected with a proportional detector.

2.8. Thermogravimetric analysis (TGA)

PS, RS, CAPS, CARS powders were dried in the oven at 105 °C for 4 h. The composites for TGA were stored in tightly sealed plastic bags for one week. Thermal properties of the powders and composites were measured with a ZTY-ZP type thermal analyzer. Sample weight varied from 10 to 15 mg. Samples were heated from room temperature to 450 °C at a heating rate of 15 °C/min in a nitrogen atmosphere.

2.9. Dynamic mechanical thermal analysis (DMTA)

The composites for DMTA were stored at 33% relative humidity (RH) for one week. The DMTA, using a Mark Netzsch DMA242 analyzer, was performed on thick specimens (40 × 7 × 2 mm) in a single cantilever-bending mode at a frequency of 3.33 Hz and a strain × 2 N, corresponding to the maximum displacement amplitude of 30 μm. The temperature range was from −100 to 100 °C. The standard heating rate used was 3.0 °C min^{-1}.

2.10. Mechanical testing

Composites were pressed with a flat sulfuration machine into a sheet. The Testometric AX M350-10KN Materials Testing Machine

was operated at a crosshead speed of 50 mm/min for tensile testing (ISO 1184–1983 standard). The data was averaged over 5–8 specimens.

In order to analyze the effect of environmental humidity on mechanical properties of the composites, they were stored in closed chambers over several aqueous mixtures at 25 °C for a period of time. The materials used were dried silica gel, $MgCl_2$ saturated solution and NaCl saturated solution, which provided RH's of 0%, 33%, and 75%, respectively.

The original water content (dry basis) of the composites were determined gravimetrically by drying small pieces of TPS at 105 °C overnight, the evaporation of glycerol was negligible (Curvelo, de Carvalho, & Agnelli, 2001). After composites had been stored for a certain period of time at RH 0% or 75%, the water contents (C) were calculated on the basis of the original weight (W_0), current weight (W) and original water content (C_0).

$$C = \frac{W - W_0(1 - C_0)}{W(1 - C_0)} \times 100\% \quad (1)$$

2.11. Water vapor permeability (WVP)

WVP tests were carried out by ASTM method E96 (1996) with some modifications (Mali, Grossmann, García, Martino, & Zaritzky, 2006). The films (about 0.5 mm thickness) were cut into circles, sealed over with melted paraffin, and stored in a desiccator at 25 °C. RH 0 was maintained using anhydrous calcium chloride in the cell. Each cell was placed in a desiccator containing saturated sodium chloride to provide a constant RH of 75%. Water vapor transport was determined by the weight gain of the permeation cell. Changes in the weight of the cell were recorded as a function of time. Slopes were calculated by linear regression (weight change vs. time) and correlation coefficients for all reported data were >0.99. The water vapor transmission rate (WVTR) was defined as the slope (g/s) divided by the transfer area (m^2). After the permeation tests, film thickness was measured and WVP (g Pa^{-1} s^{-1} m^{-1}) was calculated as:

$$\mathrm{WVP} = \frac{\mathrm{WVTR}}{P(R_1 - R_2)} \cdot x \quad (2)$$

where P is the saturation vapor pressure of water (Pa) at the test temperature (25 °C), R_1 is the RH in the desiccator, R_2, the RH in the permeation cell and x is the film thickness (m). Under these conditions, the driving force [$P(R_1-R_2)$] is 1753.55 Pa.

3. Results and discussion

3.1. Microscopy

Fig. 1 shows the FT-IR spectra of PS, RS, CAPS, and CARS powders. The characteristic peak occurred at 1650 cm^{-1}, which Fang et al. (Fang, Fowler, Tomkinson, & Hill, 2002) believed to be a feature of tightly bound water present in the starch. For CAPS and CARS powders, a new peak at 1740 cm^{-1} was characteristic of an ester group. As shown in Fig. 2, when CA was heated, it dehydrated to yield an anhydride, which could react with starch to form a starch–citrate derivative. Further heating resulted in additional dehydration with cross-linking (Wing, 1996).

Since the granules of starch were kept intact, Fig. 3a and b, the esterification step did not disrupt the starch granules. The granules of CARS were obviously smaller than those of CAPS. In Fig. 3c no residual granular structure of starch was present in the continuous TPS phase. Because of the high temperature and high shear exerted during the extrusion, and the plasticizing effect of incorporated glycerol, native pea starch granules were either molten or physically broken up after extrusion. Plasticizers are known to disrupt intermolecular and intramolecular hydrogen bonds and make the native starch plastic (Ma, Yu, & Wan, 2006). However, melt extrusion processing could not melt or break the granules of CAPS and CARS, and they were still dispersed in the CAPS/TPS and CARS/TPS composites in Fig. 3d and e. Some white circles were marked, which represented the situations of the granules and the pits in the matrix. The pits could come from the exfoliation of CARS and CAPS granules from the fracture faces when the samples were cooled in liquid nitrogen and they were broken afterward. Substitution of citric acid groups on starch chains could form a cross-linked starch, limit starch chain mobility and thus ensure the granules of CAPS and CARS as reinforcing agents in the TPS matrix.

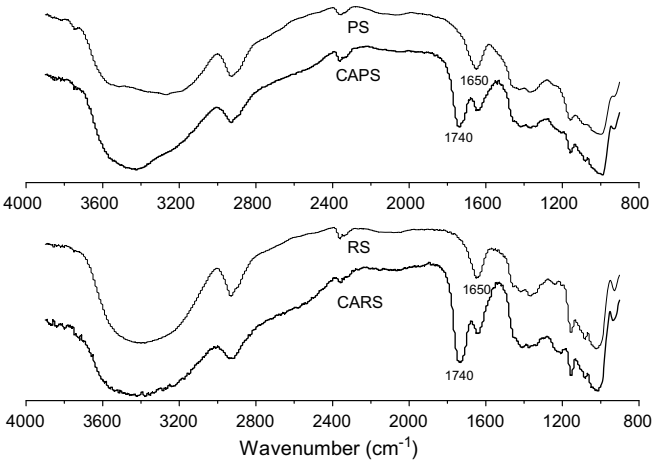

Fig. 1. The FT-IR spectra of PS, RS, CAPS, and CARS powders.

3.2. X-ray diffraction

As shown in Fig. 4a, native PS and RS possessed the A-style crystallinity, while most crystals of CAPS and CARS disappeared. When CA penetrated the starch granule, it possibly disrupted the crystalline structure of starch because of the concentrated solution of citric acid. This reaction should occur both in the amorphous phase and crystalline phase (Xie, Liu, & Cui, 2006). In TPS, CAPS/TPS and CARS/TPS composites, the V_H-style crystallinity (Fig. 4b), which was different from A-style crystallinity in native starch, originated from stress induced during thermal processing (Ma, & Yu, 2004b). According to (Van Soest, & Vliegenthart, 1997), the V_H type was a single-helical structure "inclusion complex" made up of amylose and glycerol. In addition, X-ray diffractograms indicated that the granules, Fig. 2d and e, came from CAPS and CARS, instead of PS and RS, otherwise A-style crystallinity would appear in X-ray diffractograms of CAPS/TPS and CARS/TPS composites.

3.3. TGA

In thermogravimetric analysis (TGA), the loss in mass due to volatilization of the degradation products was monitored as a function of temperature. The thermogravimetric (TG) and derivative thermogravimetric (DTG) curves of the powders, TPS, CAPS/TPS, and CARS/TPS composites are shown in Fig. 5 and Fig. 6, respectively. In Fig. 5, the mass loss of the powders was mainly ascribed to water loss before the decomposition temperature, T_{max}, which was the temperature at the maximum rate of mass loss, i.e., the peak temperature shown in DTG curves. The decomposition temperatures of PS and RS were 326.6 and 312.8 °C, while those of CAPS and CARS were 294.5 and 285.7 °C, respectively. CAPS and CARS exhibited lower thermal stability, which could be ascribed

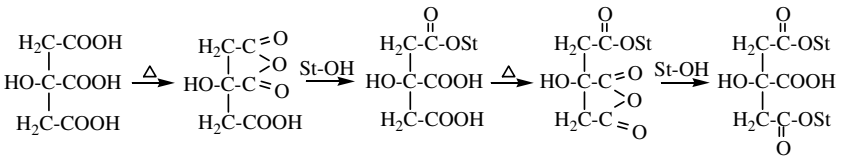

Fig. 2. Reaction scheme of citric acid with starch.

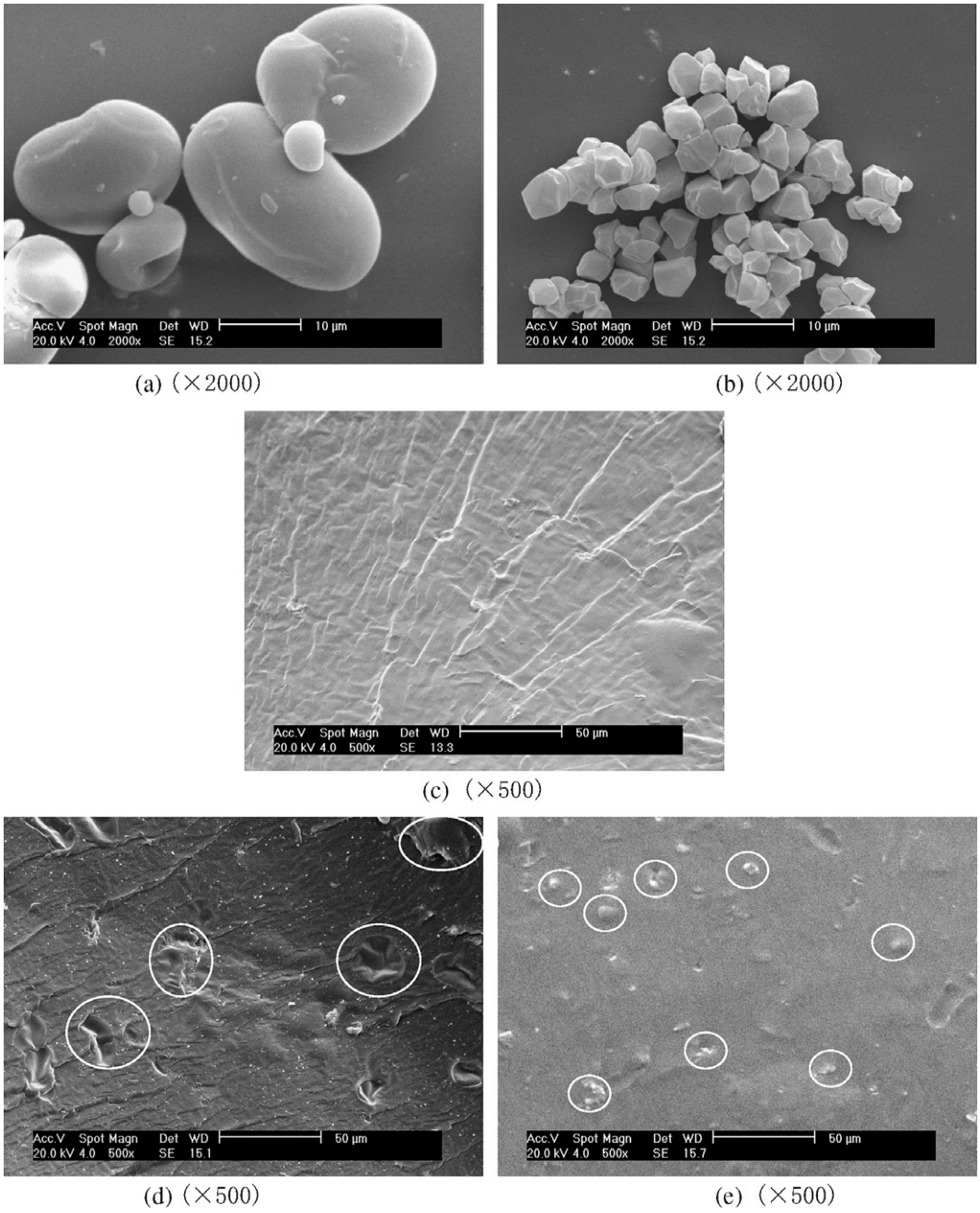

Fig. 3. SEM micrograph of CAPS (a), CARS (b) powders, the fragile fractured surface of TPS (c), CAPS/TPS composites (6 wt% CAPS) (d), and CARS/TPS composites (6 wt% CARS) (e).

to the ester bonds from the substitution that break at lower temperatures of degradation (Stojanovic, Katsikas, & Popovic, 2005).

In Fig. 6, the mass loss below 100 °C was mainly ascribed to water loss, while the mass loss before the onset temperature was related to the volatilization of both water and glycerol (Ma, Yu, & Ma, 2005). There was little difference in mass loss among TPS, CAPS/TPS, and CARS/TPS composites at onset temperature, mainly because of the similar content of water and glycerol. The degradation of TPS, CAPS/TPS, and CARS/TPS composites took place at 332.6, 322.7, and 321.6 °C, respectively. The addition of CAPS and

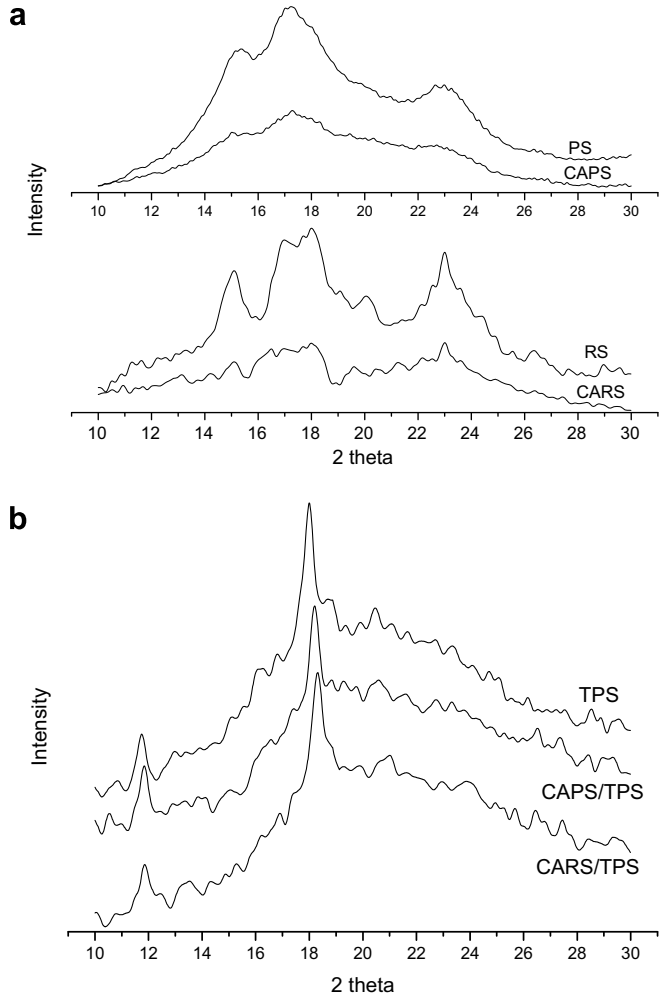

Fig. 4. The X-ray diffractograms of PS, RS, CAPS, and CARS powders (a); TPS, CAPS/TPS composites (6 wt% CAPS), and CARS/TPS composites (6 wt% CARS) (b).

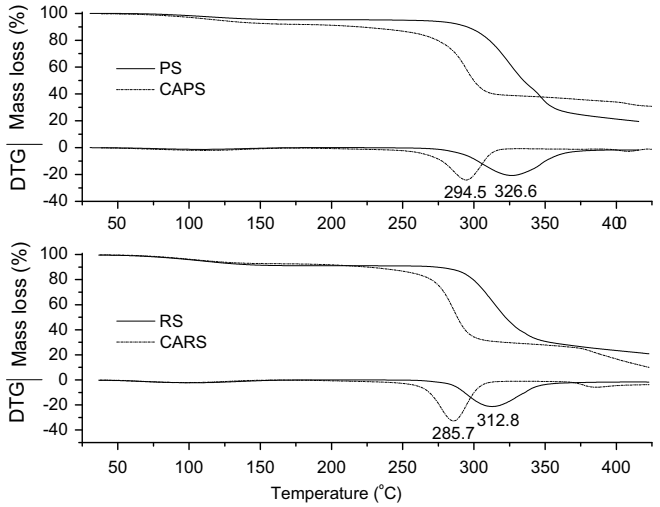

Fig. 5. Thermogravimetric curves and Derivative thermogravimetric curves for PS, RS, CAPS, and CARS powders.

CARS resulted in decreased thermal stability, which was ascribed to the lower thermal stability of CAPS and CARS.

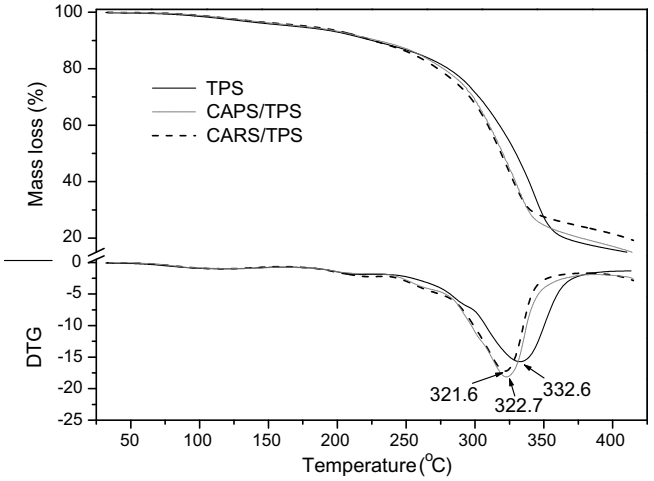

Fig. 6. Thermogravimetric curves and Derivative thermogravimetric curves for TPS, CAPS/TPS composites (6 wt% CAPS), and CARS/TPS composites (6 wt% CARS).

3.4. DMTA

As shown in Fig. 7a, the storage modulus for CAPS/TPS or CARS/TPS composites was higher than that for pure TPS. It is known that the storage modulus detected by DMTA relates to composite stiffness. The stiffness of composites increased with the introduction of CAPS or CARS granules. This improvement was possibly associated with the interaction between TPS and CAPS (or CARS). CARS granules were smaller than CAPS granules, so the stronger interface interaction between TPS and CARS made the storage modulus curve higher.

In general, the storage modulus decreased as the temperature increased. However, in the region corresponding to the maximum loss factor (tan delta) plots, the decrease in storage modulus was usually rapid. Fig. 7b shows the curves for loss factor (tan delta) as a function of temperature for CAPS/TPS or CARS/TPS composites. The loss factor was sensitive to molecular motion and its peak was related to the glass transition temperature. The curve of TPS revealed two thermal transitions. There were several different theories for the two thermal transitions of TPS. One explanation was favored in terms of the transitions corresponding to two separate phases in TPS. The upper transition (47 °C) was clearly because of a starch-rich phase, which was regarded as the glass transition temperature (T_g) of TPS materials, whereas the lower transition (−37 °C), was due to a starch-poor phase (Forssell et al., 1997).

In the CAPS/TPS and CARS/TPS composites, both the starch-rich and the starch-poor phases could form composites with CAPS or CARS, indicating that both the upper lower transitions shifted to higher temperatures. Functioning like a physical joint, CAPS or CARS improved the intermolecular interaction of TPS in the starch-rich phase, which brought adjacent chains of starch close, and hence reduced the free volume and raised the glass transitions of the composites. Since CARS granules were smaller than CAPS granules, there were more physical joints in CAPS/TPS than in CARS/TPS composites. Therefore, CARS raised the glass transition higher than CAPS.

3.5. Mechanical properties

Water sensitivity was another important criterion for many practical applications of starch products. TPS with different CAPS or CARS content levels were conditioned at different RH's (0% and 75%). Changes in the environmental humidity and storage time greatly affected the water content of TPS, which, in turn, induced

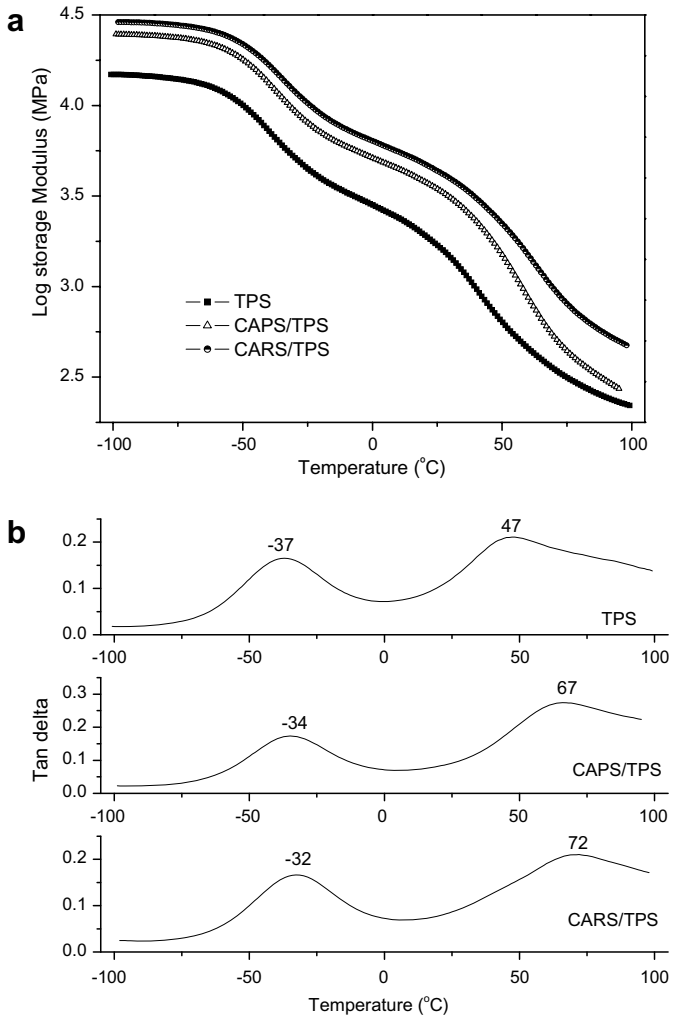

Fig. 7. Storage modulus (a) and tan delta (b) of TPS, CAPS/TPS composite (6 wt% CAPS) and CARS/TPS composite (6 wt% CARS).

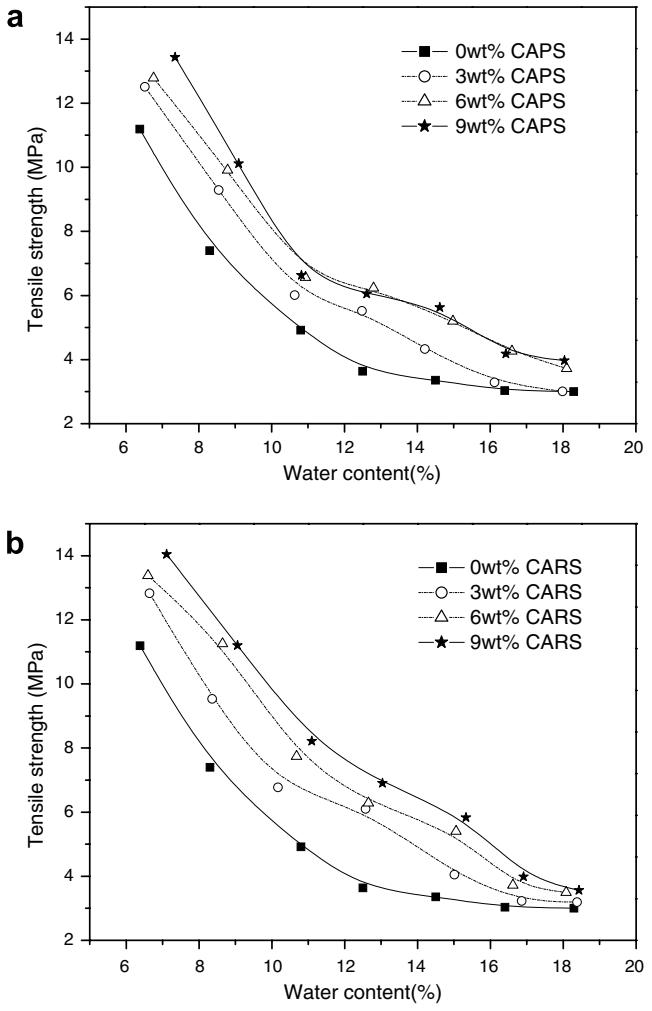

Fig. 8. The effect of CAPS, CARS, and water contents on tensile strength of CAPS/TPS (a) and CARS/TPS (b) composites.

large changes in mechanical properties. As shown in Fig. 8 and Fig. 9, the effect of different CAPS or CARS content on the mechanical properties of TPS varied with increasing water content. i.e., the elongation of all samples decreased when the water content deviated from a certain value (about 10–12%), while the materials gradually lost tensile strength as water content increased.

The higher the CAPS or CARS content was, the greater the tensile strength of the composite. The increase in tensile strength indicated that TPS was a suitable matrix for CAPS or CARS filler because of the intrinsic adhesion of the filler-matrix interface caused by the chemical similarity (polysaccharide structure) of starch and CA-modified starch. The existence of such interaction, related to the filler content, had already been confirmed by Averous, Fringant, and Moro (2001). However, the excessive CAPS (12% content) induced the conglomeration, which actually decreased the effectiveness of filler. As a result, when water content was above 10%, TPS with 12% CAPS content exhibited similar tensile strength to that with 9% CAPS, as shown in Fig. 8a.

With increasing water content, the reinforcement effect was gradually weakened, because water could separately interact with starch and CA-modified starch, and then substitute the original interaction between starch and CA-modified starch. At a high water content (>16%), the filler content would have little effect on the tensile strength, and CA-modified starch would also soften, because of water absorption. As shown in Fig. 9, when CAPS or CARS was added, the elongation at break of the composites decreased over the whole range of water content.

In addition, CARS/TPS composites had better tensile strength and elongation at break than CAPS/TPS composites with the same filler content, which was ascribed to the stronger interface interaction between TPS and the smaller CARS granules.

3.6. Water vapor permeability

As a food packaging, the film is often required to avoid or at least to decrease moisture transfer between the food and the surrounding atmosphere; water vapor permeability should be as low as possible. As shown in Fig. 10, water vapor permeability in CAPS/TPS and CARS/TPS composites showed the same trend with increasing filler content. Water vapor easily permeated TPS film with the highest WVP value at 5.01×10^{-10} g m^{-1} s^{-1} Pa^{-1}. When 3 wt% filler was added into TPS, WVP values noticeably decreased. When filler content increased, WVP values decreased gradually. At the level of 12 wt% filler, both CAPS/TPS and CARS/TPS composites showed the lowest WVP values at 2.63×10^{-10} and 2.04×10^{-10} g m^{-1} s^{-1} Pa^{-1}, respectively. Water resistance of CAPS and CARS was better than PS and RS, because the hydrophilic OH groups were substituted with hydrophobic ester groups. The addition of CAPS and CARS probably introduced a tortuous path for water molecules to pass through (Kristo & Biliaderis, 2007). At the same levels of fil-

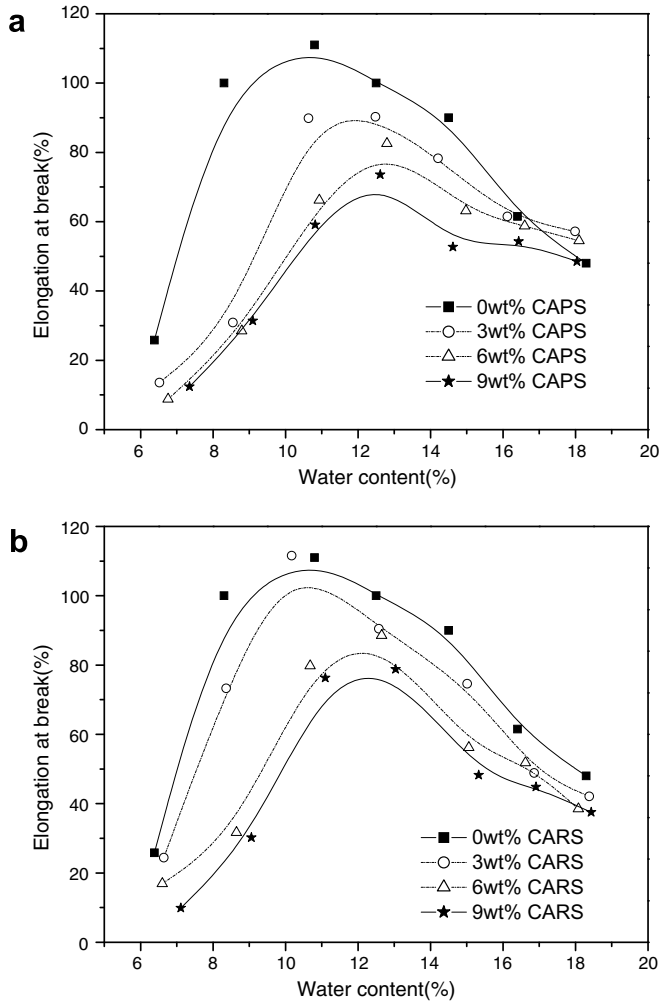

Fig. 9. The effect of CAPS, CARS, and water contents on elongation at break of CAPS/TPS (a) and CARS/TPS (b) composites.

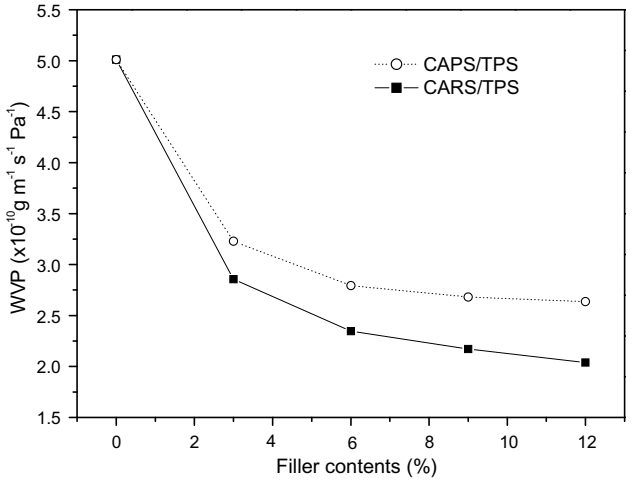

Fig. 10. The effect of CAPS and CARS contents on water vapor permeability of the composites.

ler content, CARS/TPS composites had better water vapor barrier than CAPS/TPS composites because the more numerous and smaller granules of CARS provide a more tortuous path for water molecules to follow passing through the films of CARS/TPS composites.

4. Conclusions

In this paper, biodegradable polysaccharide (CA-modified granular starch/TPS) composites were prepared as potential replacements for edible films, food packaging, biodegradable packaging, etc. The esterification of starch did not disrupt the granular structures, and the processing of melt extrusion could not melt or break the granules because of the cross-linked starch. The introduction of granular CAPS and CARS improved the storage modulus, the glass transition temperature, the tensile strength, and the water vapor barrier properties of the composites, but decreased the thermal stability. CARS/TPS composites exhibited better storage modulus, tensile strength, elongation at break and water vapor barrier than CAPS/TPS composites because of the smaller size of granular CARS.

Acknowledgement

This work was financially supported in part by Agricultural Bioproducts Innovation Program (ABIP) of Canada via the Pulse Research Network (PURENet).

References

Alvarez, V., Vázquez, A., & Bernal, C. (2005). Fracture behavior of sisal fiber-reinforced starch-based composites. *Polymer Composites, 26*, 316–323.

Angellier, H., Molina-Boisseau, S., & Dole, P. (2006). Thermoplastic starch-waxy maize starch nanocrystals nanocomposites. *Biomacromolecules, 7*, 531–539.

Averous, L., & Boquillon, N. (2004). Biocomposites based on plasticized starch: Thermal and mechanical behaviours. *Carbohydrate Polymers, 56*, 111–122.

Averous, L., Fringant, C., & Moro, L. (2001). Plasticized starch–cellulose interactions in polysaccharide composites. *Polymer, 42*, 6565–6572.

Cao, X., Chen, Y., Chang, P. R., Stumborg, M., & Huneault, M. A. (in press). Green composites reinforced with hemp nanocrystals in plasticized starch. *Journal of Applied Polymer Science*. doi:10.1002/app.28418.

Curvelo, A. A. S., de Carvalho, A. J. F., & Agnelli, J. A. M. (2001). Thermoplastic starch-cellulosic fibers composites: Preliminary results. *Carbohydrate Polymers, 45*, 183–188.

de Carvalho, A. J. F., Curvelo, A. A. S., & Agnelli, J. A. M. (2001). A first insight on composites of thermoplastic starch and kaolin. *Carbohydrate Polymers, 45*, 189–194.

Fang, J. M., Fowler, P. A., Tomkinson, J., & Hill, C. A. S. (2002). The preparation and characterisation of a series of chemically modified potato starches. *Carbohydrate Polymer, 47*, 245–252.

Fishman, M. L., Coffin, D. R., & Konstance, R. P. (2000). Extrusion of pectin/starch blends plasticized with glycerol. *Carbohydrate Polymers, 41*, 317–325.

Forssell, P. M., Mikkilä, J. M., & Moates, G. K. (1997). Phase and glass transition behaviour of concentrated barley starch–glycerol–water mixtures, a model for thermoplastic starch. *Carbohydrate Polymers, 34*, 275–282.

Funke, U., Bergthaller, W., & Lindhauer, M. G. (1998). Processing and characterization of biodegradable products based on starch. *Polymer Degradation and Stability, 59*, 293–296.

Kristo, E., & Biliaderis, C. G. (2007). Physical properties of starch nanocrystal-reinforced pullulan films. *Carbohydrate Polymers, 68*, 146–158.

Lu, Y. S., Weng, L. H., & Cao, X. D. (2006). Morphological, thermal and mechanical properties of ramie crystallites-reinforced plasticized starch biocomposites. *Carbohydrate Polymers, 63*, 198–204.

Ma, X. F., Chang, P. R., & Yu, J. G. (2008). Properties of biodegradable thermoplastic pea starch/carboxymethyl cellulose and pea starch/microcrystalline cellulose composites. *Carbohydrate Polymers, 72*, 369–375.

Ma, X. F., & Yu, J. G. (2004a). The plasticizers containing amide groups for thermoplastic starch. *Carbohydrate Polymers, 57*, 197–203.

Ma, X. F., & Yu, J. G. (2004b). The effects of plasticizers containing amide groups on the properties of thermoplastic starch. *Starch/Stärke, 56*, 545–551.

Ma, X. F., Yu, J. G., & Ma, Y. B. (2005). Urea and formamide as a mixed plasticizer for thermoplastic wheat flour. *Carbohydrate Polymers, 60*, 111–116.

Ma, X. F., Yu, J. G., & Wan, J. J. (2006). Urea and ethanolamine as a mixed plasticizer for thermoplastic starch. *Carbohydrate Polymers, 64*, 267–273.

Ma, X. F., Yu, J. G., & Zhao, A. (2006). Properties of biodegradable poly(propylene carbonate)/starch composites with succinic anhydride. *Composites Science and Technology, 66*, 2360–2366.

Mali, S., Grossmann, M. V. E., Garcıa, M. A., Martino, M. N., & Zaritzky, N. E. (2006). Effects of controlled storage on thermal, mechanical and barrier properties of plasticized films from different starch sources. *Journal of Food Engineering, 75*, 453–460.

Park, H. M., Li, X. C., & Jin, C. Z. (2002). Preparation and properties of biodegradable thermoplastic starch/clay hybrids. *Macromolecular Materials and Engineering, 287*, 553–558.

Ratnayake, W. S., Hoover, R., & Warkentin, T. (2002). Pea starch: Composition, structure and properties – A review. *Starch/Stärke, 54*, 217–234.
Sarazin, P., Li, G., & Orts, W. J. (2008). Binary and ternary blends of polylactide, polycaprolactone and thermoplastic starch. *Polymer, 49*, 599–609.
Soykeabkaew, N., Supaphol, P., & Rujiravanit, R. (2004). Preparation and characterization of jute- and flax-reinforced starch-based composite foams. *Carbohydrate Polymers, 58*, 53–63.
Stojanovic, Z., Katsikas, L., & Popovic, I. (2005). Thermal stability of starch benzoate. *Polymer Degradation and Stability, 87*, 177–182.
Van Soest, J. J. G., & Vliegenthart, J. F. G. (1997). Crystallinity in starch plastics: Consequences for material properties. *Trends in Biotechnology, 15*, 208–213.
Wilhelm, H. M., Sierakowski, M. R., & Souza, G. P. (2003). Starch films reinforced with mineral clay. *Carbohydrate Polymers, 52*, 101–110.
Wing, R. E. (1996). Starch citrate: Preparation and ion exchange properties. *Starch/Stärke, 48*, 275–279.
Xie, X. J., & Liu, Q. (2004). Development and physicochemical characterization of new resistant citrate starch from different corn starches. *Starch/Stärke, 56*, 364–370.
Xie, X. J., Liu, Q., & Cui, S. W. (2006). Studies on the granular structure of resistant starches (type 4) from normal, high amylose and waxy corn starch citrates. *Food Research International, 39*, 332–341.
Xing, G. X., Zhang, S. F., & Ju, B. Z. (2006). Microwave-assisted synthesis of starch maleate by dry method. *Starch/Stärke, 58*, 464–467.